NASA CONTRACTOR REPORT

NASA CR-500

NASA CR-500

DESIGN CONSIDERATIONS FOR THERMOSTATIC FIN SPACECRAFT TEMPERATURE CONTROL

by J. A. Wiebelt, C. A. Morgan, and G. J. Kneissl

Prepared by
OKLAHOMA STATE UNIVERSITY
Stillwater, Okla.
for

NATIONAL AERONAUTICS AND SPACE ADMINISTRATION • WASHINGTON, D. C. • MAY 1966

NASA CR-500

DESIGN CONSIDERATIONS FOR THERMOSTATIC FIN SPACECRAFT TEMPERATURE CONTROL

By J. A. Wiebelt, C. A. Morgan, and G. J. Kneissl

Prepared under Grant No. NsG-454 by
OKLAHOMA STATE UNIVERSITY
Stillwater, Okla.

for

NATIONAL AERONAUTICS AND SPACE ADMINISTRATION

For sale by the Clearinghouse for Federal Scientific and Technical Information
Springfield, Virginia 22151 – Price $2.00

INTRODUCTION

A passive-active thermal control system for use on spacecraft was described and analyzed in the previous two contractor reports, NASA CR-91 and NASA CR-155 (ref. 1,2). This control system is shown in Figure 1 and consists of a finned surface which has fins made of thermostatic material. The basic concept of operation of the control system is that the fins will react to their local temperature causing a variation in the ratio of the solar absorptance to the terrestial emittance. → 32

to p. 32

Two fin positions describe the limits on the α_s/ϵ_t ratio which may be obtained. These two positions are shown in Figure 2. In the open position the α_s/ϵ_t ratio depends on the spacecraft surface coating and the coating on the inner surfaces of the fins. For the closed position, the α_s/ϵ_t ratio depends on the coating used for the back or outer surface of the fins. One other controllable variable in the limiting value of the α_s/ϵ_t values is the fin spacing ratio H/W as shown in Figure 1.

Analysis of the groove formed by the fins' inner surface and the spacecraft skin when the fins are in the open position was reported in NASA CR-91 (ref. 1) assuming that the skin coating is a diffuse reflector and the fin inner surfaces are specular reflectors. These results are shown in Figures 3, 4, and 5 for three values of H/W. In order to present this information in the most usable format the ratio of the effective reflectance ρ_e to the reflectance of the skin coating ρ_b is shown as a function of solar polar angle φ (see Figure 2) with the fin inner surface reflectance, ρ_w, as a parameter. Since this is the typical position of the fins when in sun irradiation, the curves may be used to determine the solar absorptance for various combinations of base coating, fin coating, and fin spacing ratio. Figures 3, 4, and 5 were prepared assuming the length of the groove formed by the fins and the spacecraft skin was infinite. In order to assess the effect of a finite length for the groove, similar curves are presented from NASA CR-155 (ref. 2) in Figures 6 and 7 for ratios of length D (see Figure 1) to fin height H equal to 5 and 25.

In the fin open position, the terrestial emittance is also required. This quantity was also reported in NASA CR-155 (ref. 2). In this case the emittance factor was defined rather than the effective emittance. In this analysis the emittance factor was defined as the ratio of all the energy leaving a finite length groove to the energy which would leave a black surface which had an area equal to the spacecraft skin area. Since energy is also emitted by the fins, the emittance factor can be a value larger than unity. However, this is the quantity required by a designer, since the energy flux leaving the spacecraft skin is normally required. The results of these calculations are shown in Figures 8 and 9 with emittance factor plotted as a function of fin inner surface reflectance with the spacecraft skin coating emittance as a parameter. In these two sets of curves it was assumed that the spacecraft skin temperature and the fin temperature were equal. This assumption is not valid but may represent a reasonable approximation for this case.

The other limiting value of the α_s/ϵ_t ratio would occur with the fins in the closed position as shown in Figure 2 - part b. When in this position, the

NASA SPACECRAFT THERMOSTAT SURFACE

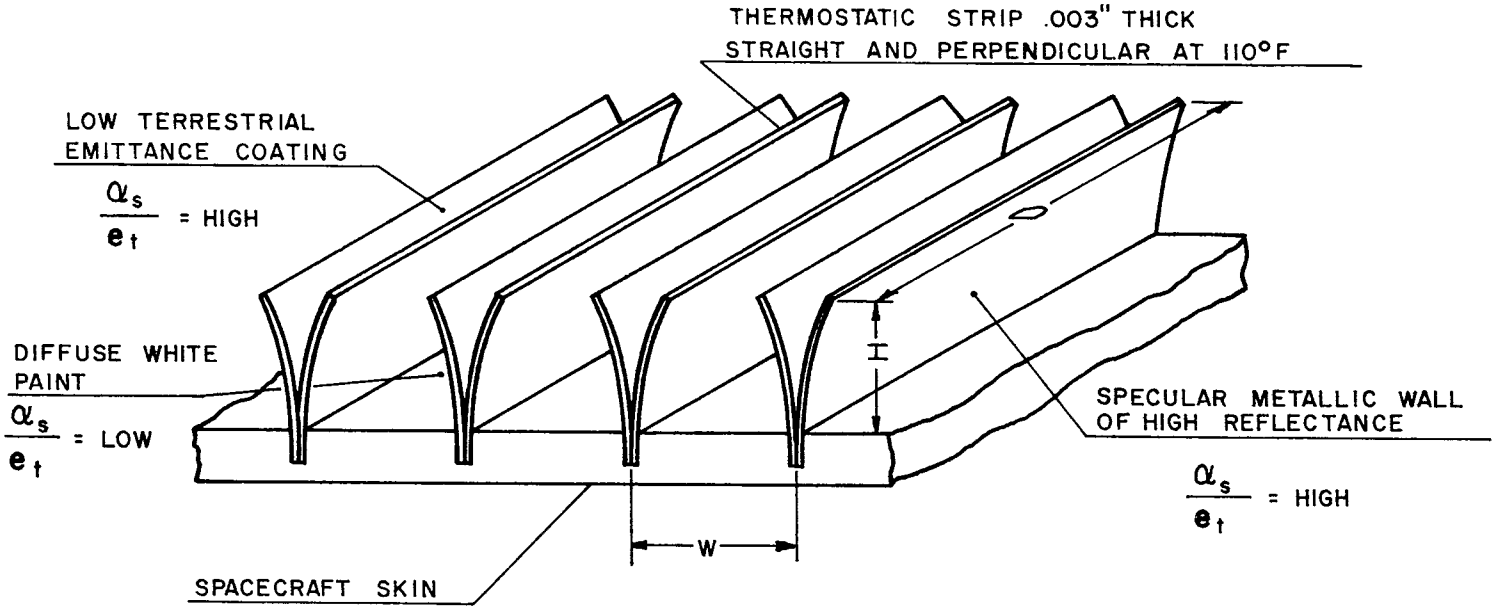

Figure (1)

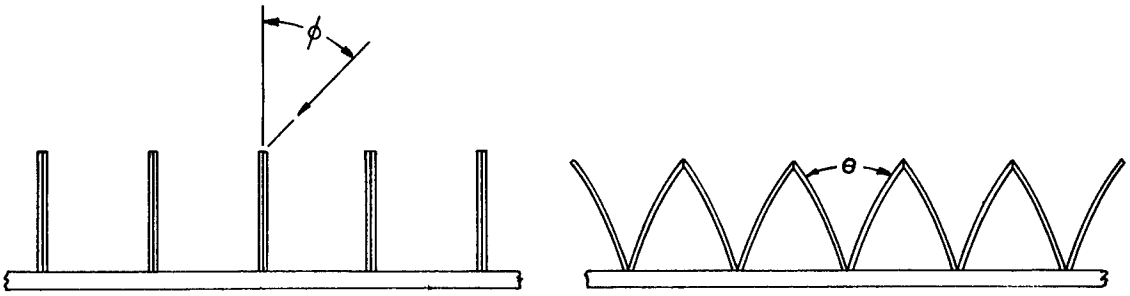

(a) Fins Open (b) Fins Closed

Figure (2) Extreme Positions of Fins.

entire spacecraft skin is shielded by the infinite length fins and may be effectively shielded in the finite length case by end closures. Since this position occurs primarily with no solar irradiation, the terrestial emittance is the primary variable required for analysis. This value is considered in the next section.

Emittance of Fins in Closed or Partially Closed Position

When the fins are in the closed or partially closed position, the back surface of the two fins at a given position forms a V-groove. This V-groove has a maximum total included angle θ of 60° (see Figure 2) when the H/W ratio is one. For other H/W ratios the maximum angle will be greater or smaller than 60°; however for practical geometries, they are most likely to be less than 60°. When in the closed position, the fins approximate a specular V-groove enclosure since the radius of curvature for the fins is large compared to fin length. Fin material as supplied has a smooth rolled metal surface which for the long wave emission to be considered is more nearly specular than diffuse.

An analysis of specular V-groove surfaces for absorptance has been presented to NASA by E. M. Sparrow and S. H. Lin (ref. 3). The results presented in this paper were not of sufficient range for use with highly reflecting materials or for groove angles less than 30°. For this reason the analysis was extended resulting in the following two expressions:

for $\frac{360°}{\theta}$ even, with $n = \frac{180°}{\theta}$

$$\alpha_a = 1 - \frac{2\left(1 - \cos\frac{\theta}{2}\right)}{\sin\frac{\theta}{2}} \left\{ \sum_{k=1}^{n-1} \rho^k \sin k\frac{\theta}{2} + \frac{1}{2}\rho^n \right\} \qquad (1)$$

Effective Reflectance Ratio

H/W = 0.667

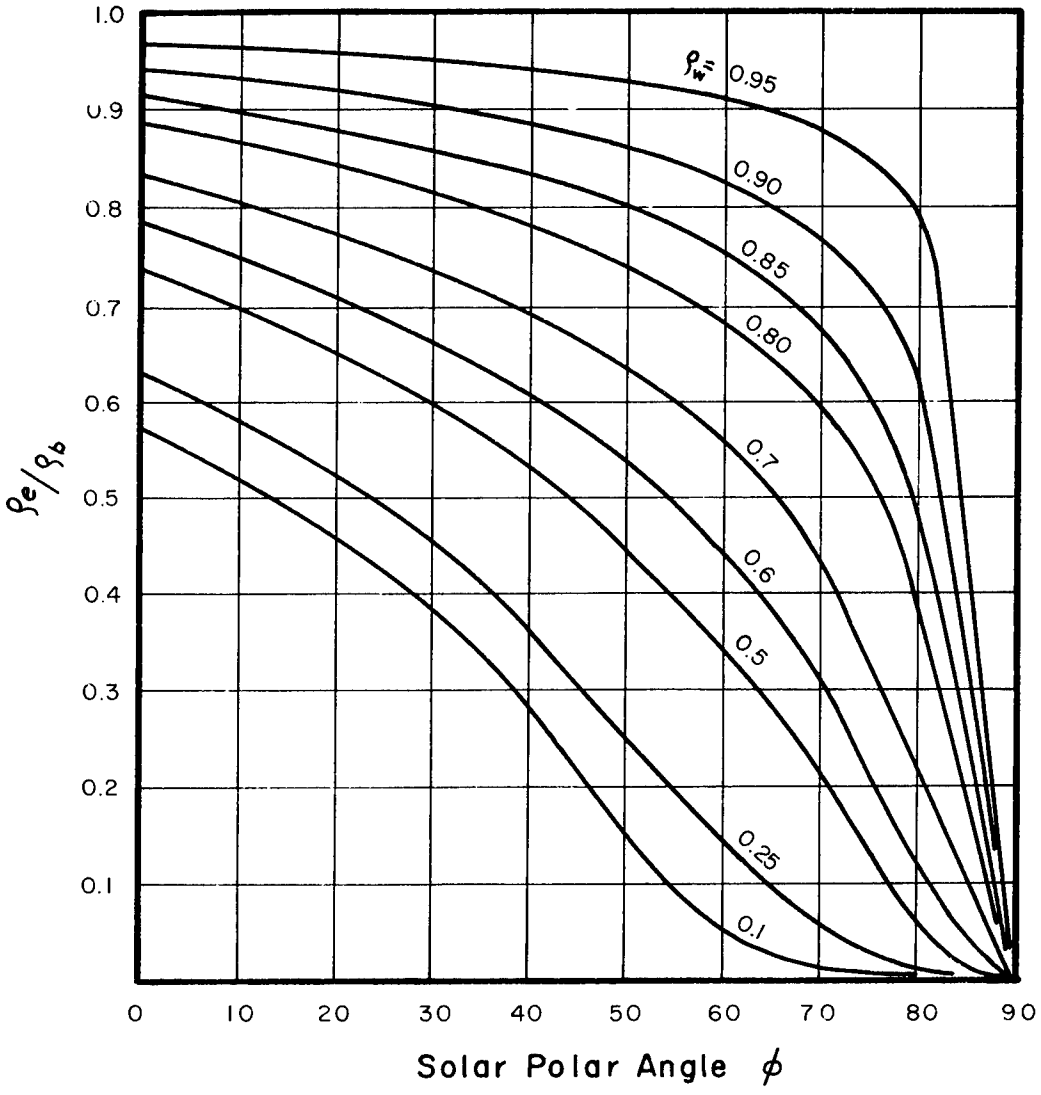

Figure (3)

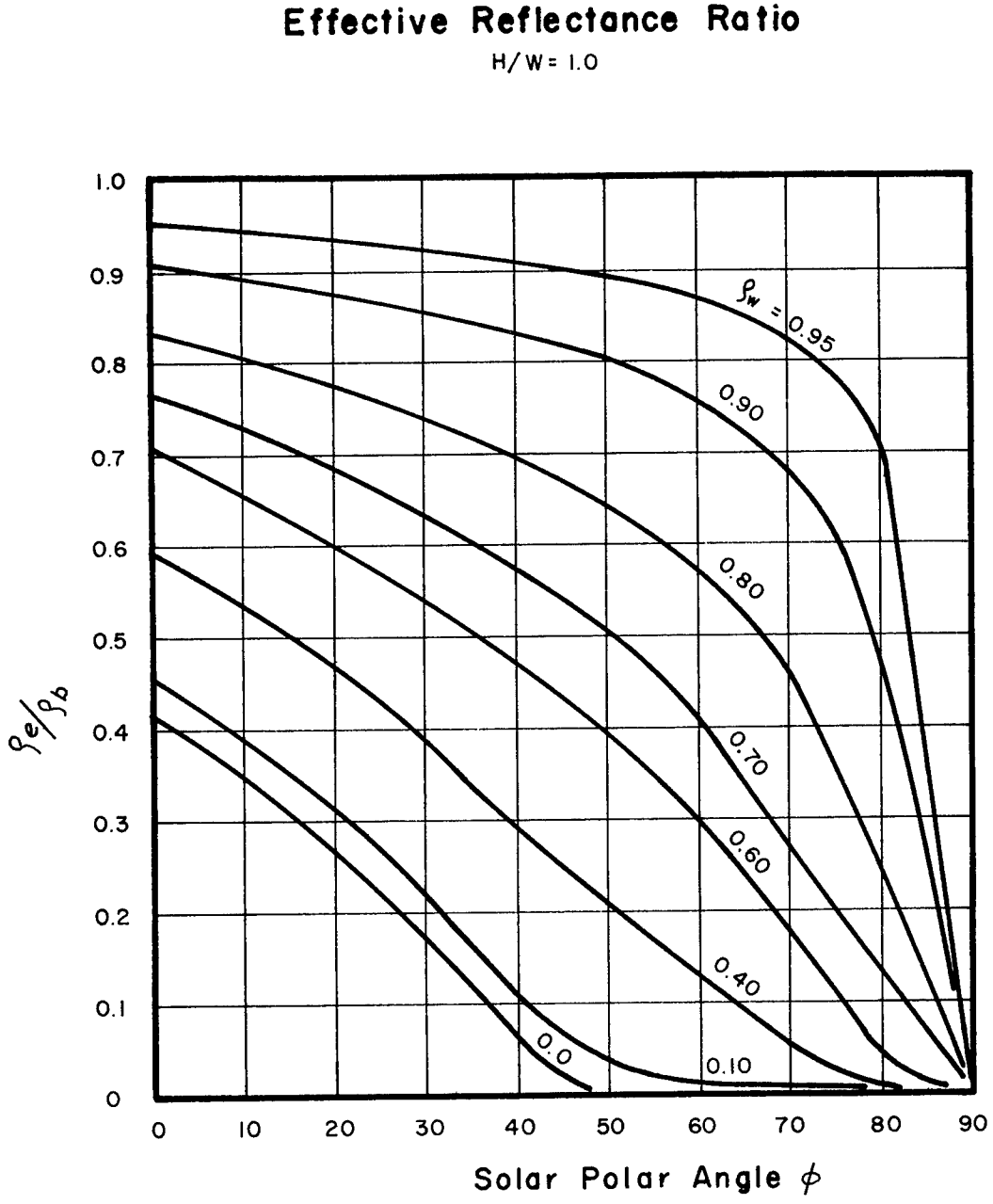
Effective Reflectance Ratio
H/W = 1.0
1.0
0.9
0.8
0.7
0.6
0.5
0.4
0.3
0.2
0.1
0
ρ_e/ρ_b
ρ_w = 0.95
0.90
0.80
0.70
0.60
0.40
0.10
0.0
0
10
20
30
40
50
60
70
80
90
Solar Polar Angle ϕ

Figure (4)

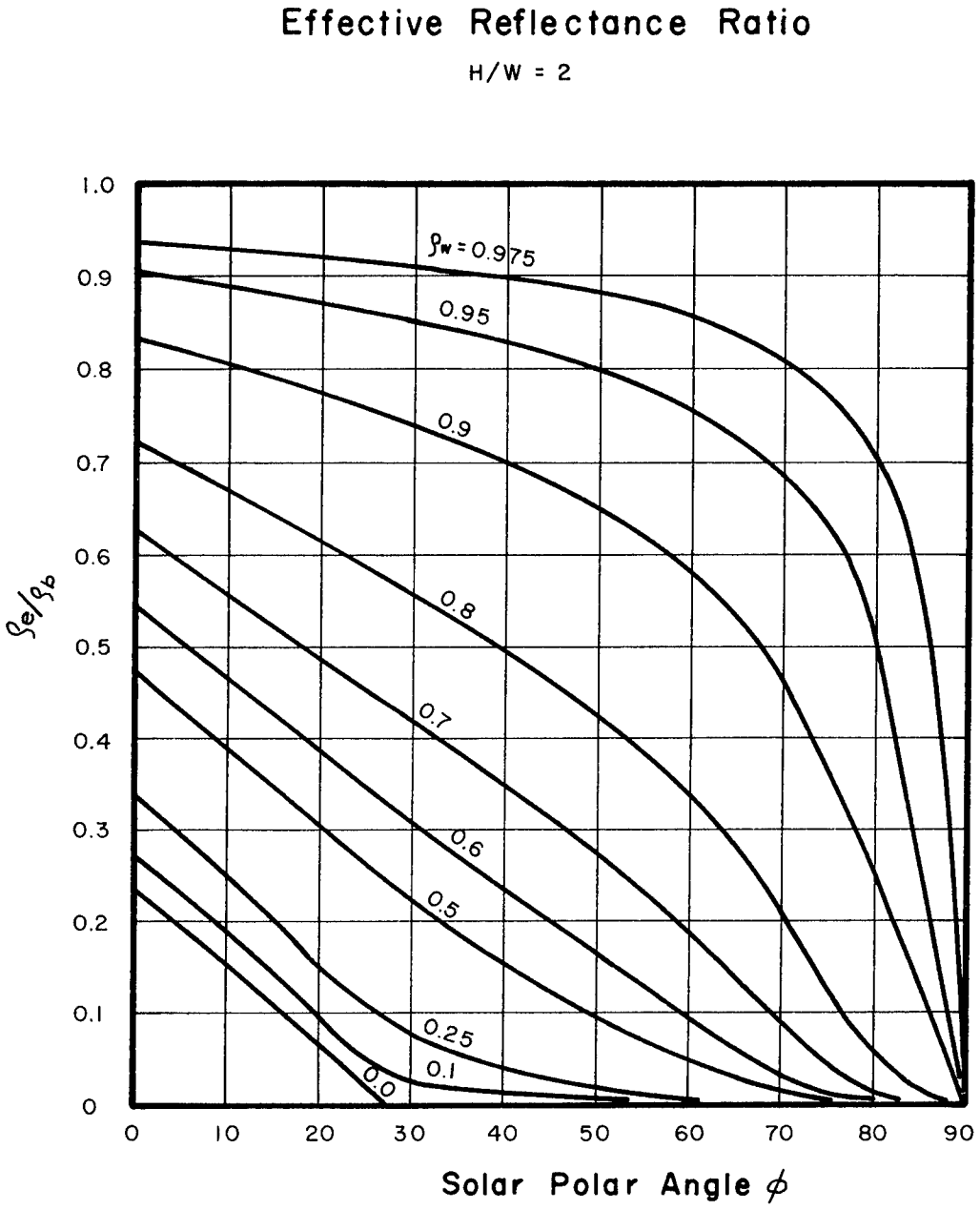
Effective Reflectance Ratio
H/W = 2
1.0
0.9
0.8
0.7
0.6
0.5
0.4
0.3
0.2
0.1
0
ρe/ρb
ρw = 0.975
0.95
0.9
0.8
0.7
0.6
0.5
0.25
0.1
0.0
0
10
20
30
40
50
60
70
80
90
Solar Polar Angle φ

Figure (5)

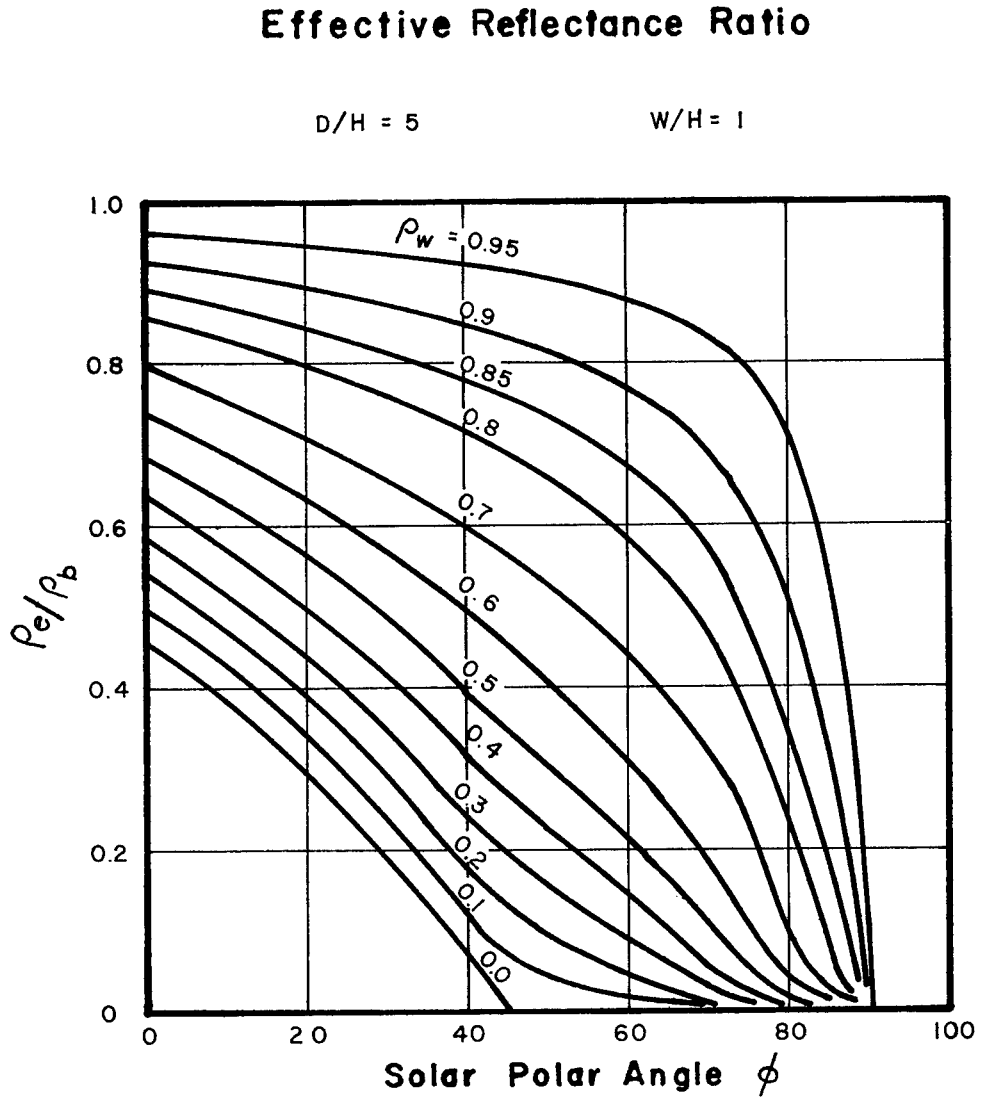
Effective Reflectance Ratio
D/H = 5
W/H = 1
ρ_w = 0.95
0.9
0.85
0.8
0.7
0.6
0.5
0.4
0.3
0.2
0.1
0.0
ρ_e/ρ_b
1.0
0.8
0.6
0.4
0.2
0
0
20
40
60
80
100
Solar Polar Angle ϕ

Figure (6)

Effective Reflectance Ratio

D/H = 25 W/H = 1

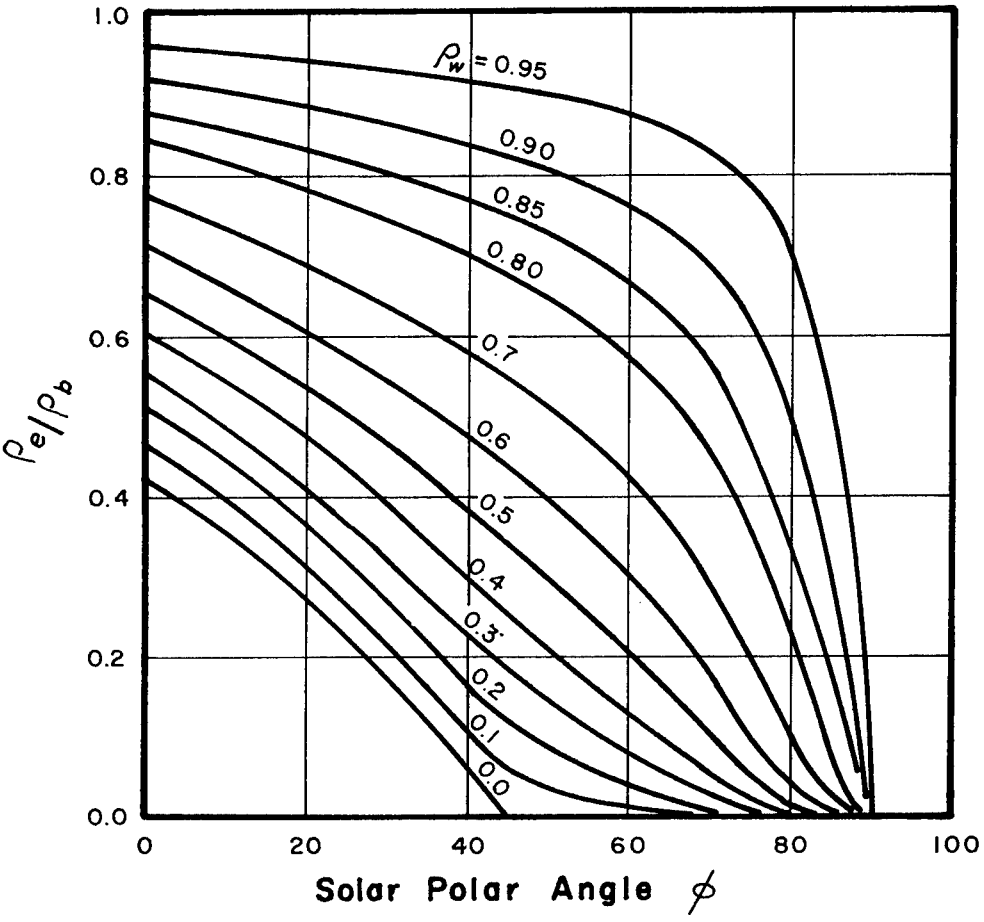

Figure (7)

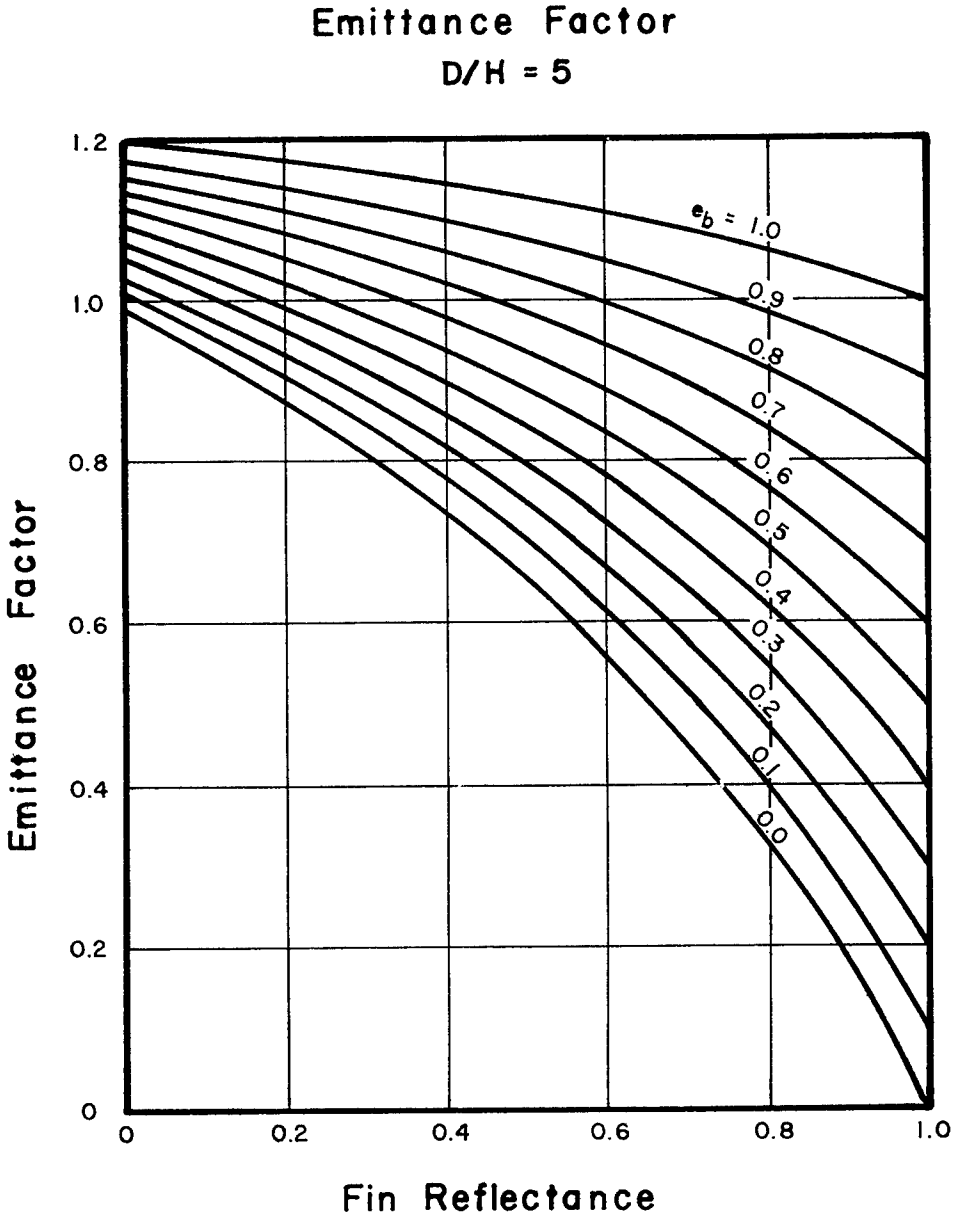
Emittance Factor
D/H = 5
1.2
1.0
0.8
0.6
0.4
0.2
0
Emittance Factor
e_b = 1.0
0.9
0.8
0.7
0.6
0.5
0.4
0.3
0.2
0.1
0.0
0
0.2
0.4
0.6
0.8
1.0
Fin Reflectance

Figure (8)

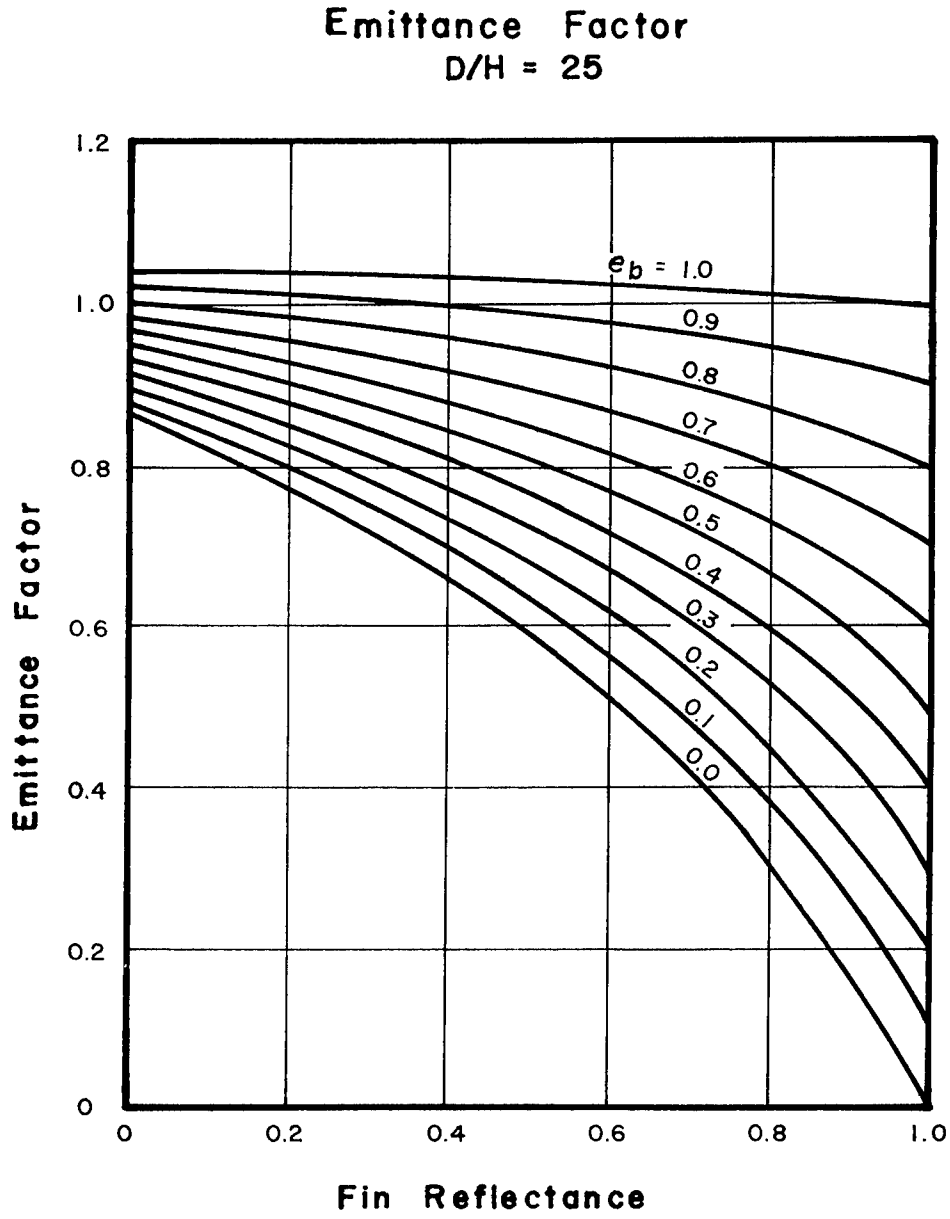
Emittance Factor
D/H = 25
1.2
1.0
0.8
0.6
0.4
0.2
0
Emittance Factor
e_b = 1.0
0.9
0.8
0.7
0.6
0.5
0.4
0.3
0.2
0.1
0.0
0
0.2
0.4
0.6
0.8
1.0
Fin Reflectance

Figure (9)

and for $\frac{360°}{\theta}$ odd, with $n = \frac{1}{2}\left(\frac{360°}{\theta} - 1\right)$

$$\alpha_a = 1 - \frac{2\left(1 - \cos\frac{\theta}{2}\right)}{\sin\frac{\theta}{2}} \sum \rho^k \sin k\frac{\theta}{2} \qquad (2)$$

Equations (1) and (2) are to be used only for the cases of $360°/\theta$ an even or odd integer and for infinite length grooves.

The value of the apparent absorptance given in equations (1) and (2) can be interpreted as the apparent emittance if the value of the reflectance ρ is replaced with $1 - \varepsilon$ where ε is the emittance of the surface of the V-groove. In this case the meaning is that the area of the top of the groove or the groove opening will have an effective emittance as given if the walls of the groove are at a constant and uniform temperature T. The results as given by equations (1) and (2) are plotted in Figure 10.

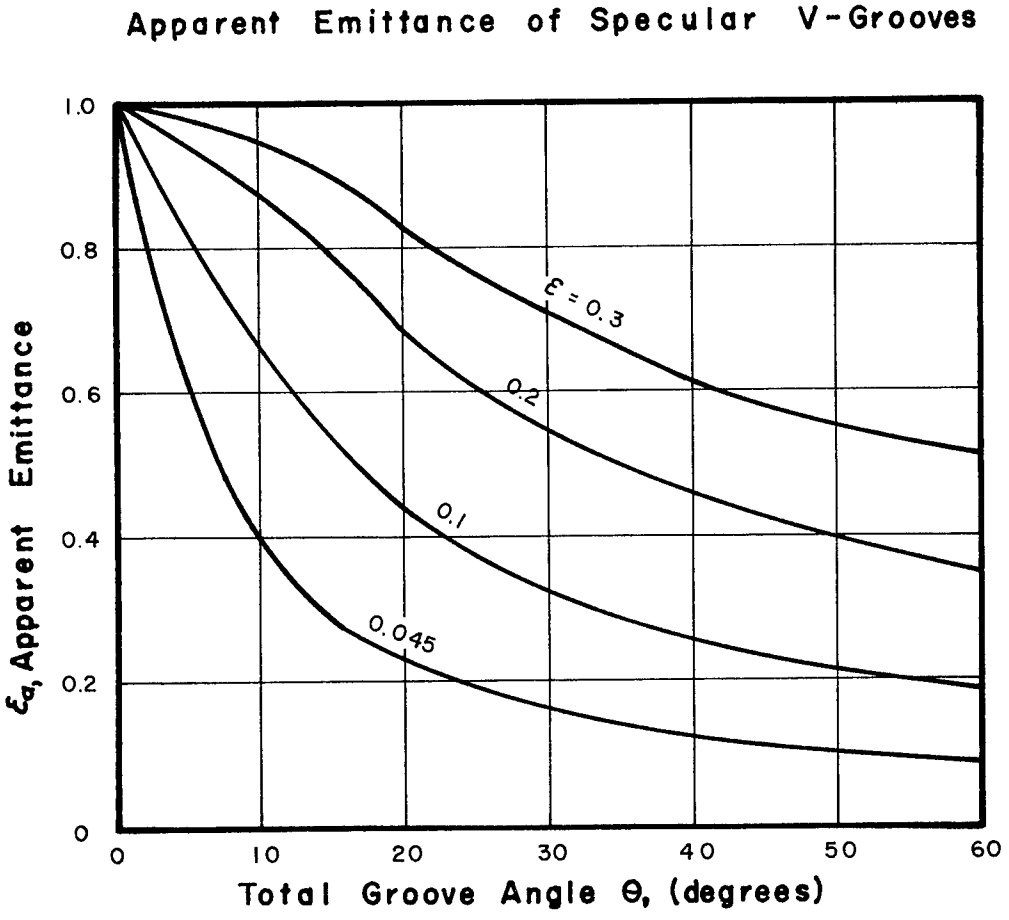

Figure (10)

SUGGESTED DESIGN TECHNIQUE

It will be assumed that the spacecraft designer has available the following design criteria:

1. Energy flux to be radiated to space q''_s in Btu/hr - ft^2
2. Spacecraft skin temperature T_s in °R
3. Solar constant G_s in Btu/hr - ft^2.

Of course, any or all of these may be variable during a mission. It is recommended that the expected values be searched and from the expression

$$e'_r = \frac{q''_s}{\sigma T_s^4} \tag{3}$$

the largest value of e'_r be determined. This value of e'_r will be one limit which specifies the material coatings required for the spacecraft skin and fins. As shown in NASA CR-91 (ref. 1)

$$e'_r = \epsilon_t - \alpha_s \left(\frac{G_s}{\sigma T_s^4} \right) \tag{4}$$

so with e'_r maximum known and G_s maximum known, the terrestial emittance and solar absorptance values are related. From the known types of base coatings available (white paints of various types) the values of ϵ_t and α_s for possible coatings may be used with Figures 3 through 9 to determine the reflectance required for the fin inner surface. Conversely, for known coating materials, the figures plus equation (4) may be used to determine the spacecraft skin temperature T_s when the fins are wide open.

Thermal Model of Thermostatic Finned Surface

In the overall thermal analysis of a spacecraft, a thermal model is usually required for each element of the system. The thermal model for the finned surface may be determined as follows. It is assumed that thermal conductance and thermal capacitance are the values required for the model.

The geometry for the calculation of the conductances of the inner surfaces is shown in Figure 11. The following assumptions were made:

(a) The system has infinite length normal to Figure 11.
(b) The fins are specular reflectors and diffuse emitters.
(c) The base or spacecraft skin is a diffuse reflector and a diffuse emitter.
(d) The fins have a straight profile rather than a curved profile.

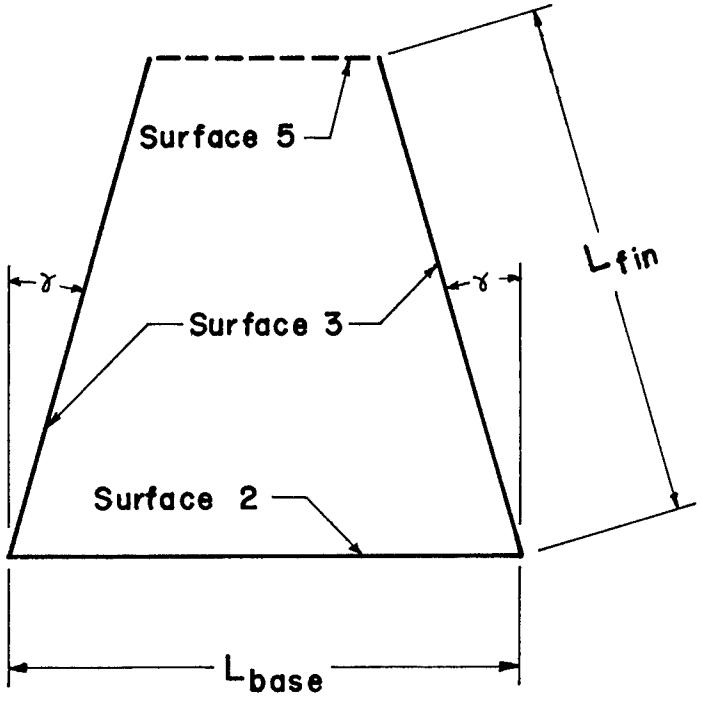

Figure (11) Geometry for Inner Surface Conductances.

(e) The base and fin temperatures can be represented as a uniform and constant value, i.e., each surface can be represented as a single temperature node.

In the usual thermal analysis the energy exchange between two nodes in the system is expressed as $q_{ij} = K_{ij} (T_i - T_j)$, where K_{ij} is the conductance between the two nodes. For this model the energy exchange between nodes will be by both conduction and radiation. The conduction transfer is relatively well known and will be considered last. For the radiation transfer, the basic method of H. C. Hottel was used. This method uses $q_{ij} = \mathcal{F}_{ij} A_i (E_{bi} - E_{bj})$ for the radiant energy exchange between surfaces. In the expression $\mathcal{F}_{ij}$ is the radiant exchange factor, A_i is the surface area of surface i, and E_{bi} is the total emissive power of a black body at the temperature of surface i. By equating the linear conductance equation and Hottel's expression for q_{ij}, the conductance for radiant exchange is given by equation (5),

$$K_{ij} = \mathcal{F}_{ij} A_i \sigma \left(T_i^2 + T_j^2\right)\left(T_i + T_j\right) \qquad (5)$$

In equation (5) the only quantity which must be obtained for most thermal analyses is $\mathcal{J}_{ij}$ or the $\mathcal{J}_{ij}A_i$ product.

Evaluation of $\mathcal{J}_{ij}$ for the Thermal Model

The evaluation of $\mathcal{J}_{ij}$ for a specular system was done using the image method as presented by Eckert and Sparrow (ref. 4) using a two bounce or two image limit. This analysis could be made more accurate by using more images but the increase in accuracy is not justified considering the lack of precision in property evaluation.

For the two bounce approximation the fin system of Figure 11 with two images is shown in Figure 12. In this case the two opposed fins are numbered 3 and $\bar{3}$

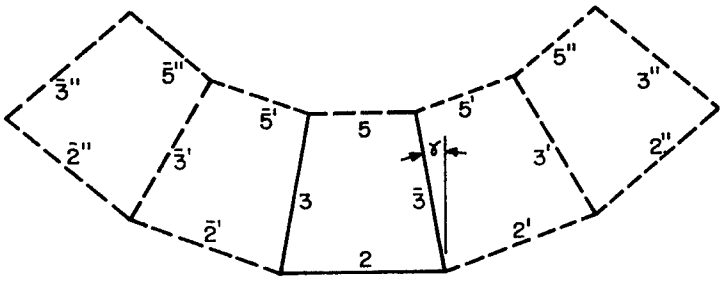

Figure (12) Fin System with Two Images.

respectively to indicate the method of analysis. The basic quantities required to obtain the $\mathcal{J}_{ij}$ values are the irradiation equations following.

$$G_2A_2 = E_3A_3\left[F_{32} + \rho_{\bar{3}}\,F_{3'2} + \rho_{\bar{3}}\rho_3\,F_{3''2}\right] + E_{\bar{3}}A_{\bar{3}}\left[F_{\bar{3}2} + \rho_3\,F_{\bar{3}'2} + \rho_3\rho_{\bar{3}}\,F_{\bar{3}''2}\right] + J_2A_2\left[\rho_3\,F_{\bar{2}'2} + \rho_{\bar{3}}\,F_{2'2} + \rho_3\rho_{\bar{3}}\,F_{\bar{2}''2} + \rho_3\rho_{\bar{3}}\,F_{2''2}\right] \quad (6)$$

$$G_3A_3 = E_3A_3\left[\rho_{\bar{3}}\,F_{3'3}\right] + E_{\bar{3}}A_{\bar{3}}\left[F_{\bar{3}3} + \rho_3\rho_{\bar{3}}\,F_{\bar{3}''3}\right] + J_2A_2\left[F_{23} + \rho_{\bar{3}}\,F_{2'3} + \rho_3\rho_{\bar{3}}\,F_{2''3}\right] \quad (7)$$

$$G_5A_5 = E_3A_3\left[F_{35} + \rho_{\bar{3}}\, F_{3'5} + \rho_3\rho_{\bar{3}}\, F_{3''5}\right]$$

$$+ E_{\bar{3}}A_{\bar{3}}\left[F_{\bar{3}5} + \rho_3\, F_{\bar{3}'5} + \rho_3\rho_{\bar{3}}\, F_{\bar{3}''5}\right]$$

$$+ J_2A_2\left[F_{25} + \rho_3\, F_{\bar{2}'5} + \rho_{\bar{3}}\, F_{2'5} + \rho_3\rho_{\bar{3}}\, F_{\bar{2}''5} + \rho_3\rho_{\bar{3}}\, F_{2''5}\right] \quad (8)$$

where

G_i is the irradiation of surface i.

E_i is the total emissive power of surface i.

ρ_i is the reflectance of surface i.

F_{ij} is the diffuse configuration factor from surface i to surface j.

Equations (6), (7), and (8) can be written in a much more compact form if the multipliers of the E_iA_i and J_iA_i terms are denoted as $F_{ij\ tot}$, where i represents the radiating node and j represents the irradiated node, e.g., in equation (6)

$$F_{32\ tot} = F_{32} + \rho_{\bar{3}}\, F_{3'2} + \rho_{\bar{3}}\rho_3\, F_{3''2}$$

would be used. Rewriting equations (6), (7), and (8) in this form results in the following irradiation equations:

$$G_2A_2 = E_3A_3\, F_{32\ tot} + E_{\bar{3}}A_{\bar{3}}\, F_{\bar{3}2\ tot} + J_2A_2\, F_{22\ tot} \quad (9)$$

$$G_3A_3 = E_3A_3\, F_{33\ tot} + E_{\bar{3}}A_{\bar{3}}\, F_{\bar{3}3\ tot} + J_2A_2\, F_{23\ tot} \quad (10)$$

$$G_5A_5 = E_3A_3\, F_{35\ tot} + E_{\bar{3}}A_{\bar{3}}\, F_{\bar{3}5\ tot} + J_2A_2\, F_{25\ tot} \quad (11)$$

Evaluation of the script $\mathcal{F}$ or radiant transfer functions was accomplished using the net heat transfer equations as follows. The basic equations for energy transfer are given as either

$$q''_jA_j = G_jA_j - J_jA_j \quad (12)$$

or

$$q''_jA_j = \alpha_jG_jA_j - E_jA_j \quad (13)$$

If q_{ij} is to be evaluated, equations (12) and (13) may be used with surface i an energy source and all other surfaces receivers. This is accomplished

analytically by setting $E_{bi} = 1.0$ and all other E_b values at zero. For example:

$$q_{ij} = q''_{ij}A_i = \mathcal{J}_{ij}A_i \ (1.0 - 0.0) \tag{14}$$

and

$$q''_{ij}A_i = \alpha_i G_i A_i - E_i A_i \tag{15}$$

where G_iA_i is determined using $E_{bi} = 1.0$ and all other E_b values equal zero.

Using this technique with equations (9), (10), (11), (12), and (13) the radiant transfer functions were determined to be:

$$\mathcal{J}_{23} = \frac{\alpha_3 \ \epsilon_2 \ F_{23\ tot}}{1 - \rho_2 \ F_{22\ tot}} \tag{16}$$

$$\mathcal{J}_{25} = \frac{\epsilon_2 \ F_{25\ tot}}{1 - \rho_2 \ F_{22\ tot}} \tag{17}$$

$$\mathcal{J}_{35} = \epsilon_3 \ F_{35\ tot} + \frac{\epsilon_3 \ \rho_2 \ F_{25\ tot}}{1 - \rho_2 \ F_{22\ tot}} \tag{18}$$

The evaluation of these equations was carried out assuming that the surface 5 was a perfect window, i.e., $\epsilon_5 = 1.0$ and $T_5 = 0$.

In order to evaluate the energy loss by the back of a fin to the surroundings the following reasoning was used. The back of two fins forms a V-groove with the groove opening equal to $2A_3 \sin \frac{\theta}{2}$ or $2A_3 \sin \gamma$. The energy loss through this area is given by $\epsilon_a E_{b3} \ (2A_3 \sin \gamma)$ where ϵ_a is the apparent emittance of the groove. Then the energy loss from the back of a single fin is $\epsilon_a E_{b3} A_3 \sin \gamma$. Equating this to q_{34} where the window over the groove is identified as surface 4 to differentiate the energy flow from inner or outer surfaces of the fin, the result is,

$$\mathcal{J}_{34} = \epsilon_a \sin \gamma \tag{19}$$

Equations (16), (17), (18), and (19) relate the diffuse energy radiant transfer functions necessary to evaluate the low temperature or terrestial energy exchange in the fin system. Since the solar energy incoming to the system will be collimated or directional, a different approach must be taken for these energy gains.

Solar Energy Fluxes

The following derivations and discussions assume normal incidence of the solar energy.

Figure 13 shows the geometry considered for the evaluation of the solar energy input to the fin system. As may be noted, the analysis assumes that the two fins on either side of the base area A_2 have moved inward symmetrically. This will be true only for normal incidence solar energy.

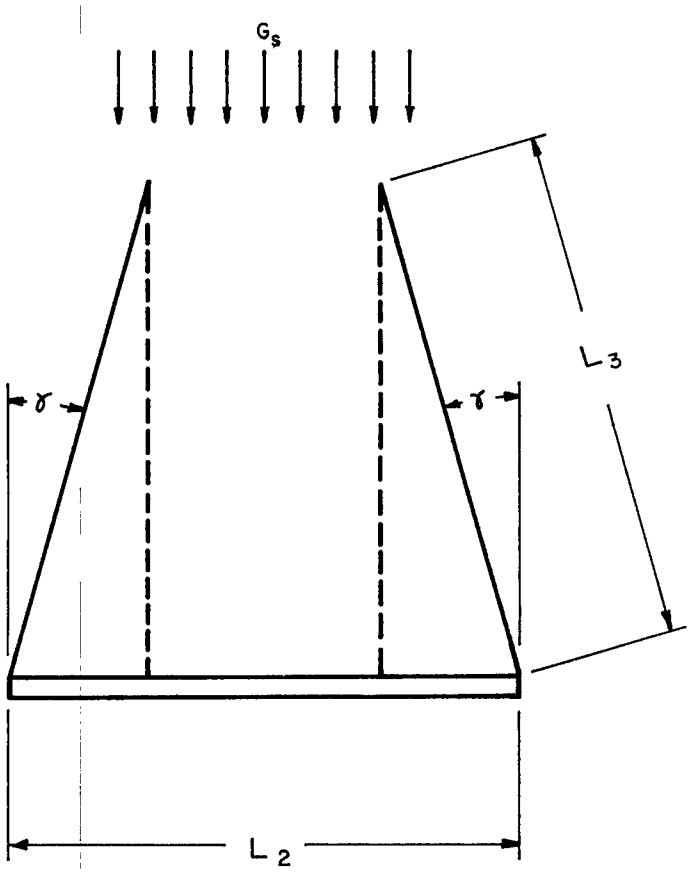

Figure (13) Geometry for Solar Flux Evaluation.

In this case, the solar energy incident upon surface 2 per unit length is G_s $(L_2 - 2L_3 \sin \gamma)$. Since we are considering the solar energy separate from the

terrestial energy, the radiosity of surface 2 may be written as $J_2A_2 = \rho_2 G_2 A_2$ where the emitted portion is considered to be zero in these wave lengths. Then using our previously obtained configuration factors we can write the total irradiation of surface 2 as the sum of the solar irradiation plus the energy reflected back to surface 2 from the solar irradiation.

$$G_2A_2 = G_s (L_2 - 2L_3 \sin \gamma)(\text{unit depth}) + J_2A_2 F_{22\ tot}.$$

Finally using $J_2A_2 = \rho_2 G_2 A_2$, the total irradiation is given by the following:

$$G_2A_2 = \frac{G_s (L_2 - 2L_3 \sin \gamma)(\text{unit depth})}{1 - \rho_2 F_{22\ tot}} \tag{20}$$

In equation (20) the value of reflectance ρ_2 and other reflectances in $F_{22\ tot}$ are reflectances to solar energy or $(1 - \alpha_s)$. Then the total solar energy absorbed by the surface 2 is given by $Q_{sol.2} = \alpha_2 G_2 A_2$ or per unit length as

$$Q_{sol.2} = \frac{G_s \alpha_2 [L_2 - 2L_3 \sin \gamma]}{1 - \rho_2 F_{22\ tot}} \tag{21}$$

By the same reasoning process the solar energy absorbed by the inner surface of the fins is given by

$$Q_{sol.3\ inner} = \frac{\rho_2 [L_2 - 2L_3 \sin \gamma] F_{23\ tot} \alpha_{3\ inner}}{1 - \rho_2 F_{22\ tot}} \tag{22}$$

In equation (22) $\alpha_{3\ inner}$ is the solar absorptance of the material on the inside of the fin or the side facing A_2. This surface may be any vacuum plated surface or the "as received" inner surface of the fins. Typically this is the low expansion material of the bimetallic fin material.

The solar energy absorbed by the outer surface or back of a fin is obtained directly from the apparent absorptance curves and is given by

$$Q_{sol.3\ outer} = G_s \alpha_{3\ outer} L_3 \sin \gamma \tag{23}$$

where $\alpha_{3\ outer}$ is the apparent absorptance of the V-groove obtained from Figure 14 using the solar absorptance of the outer fin surface obtained from monochromatic reflectance measurement.

Preparation of the Thermal Model for the Experimental System

After the derivations of the previous two sections were completed, a thermal

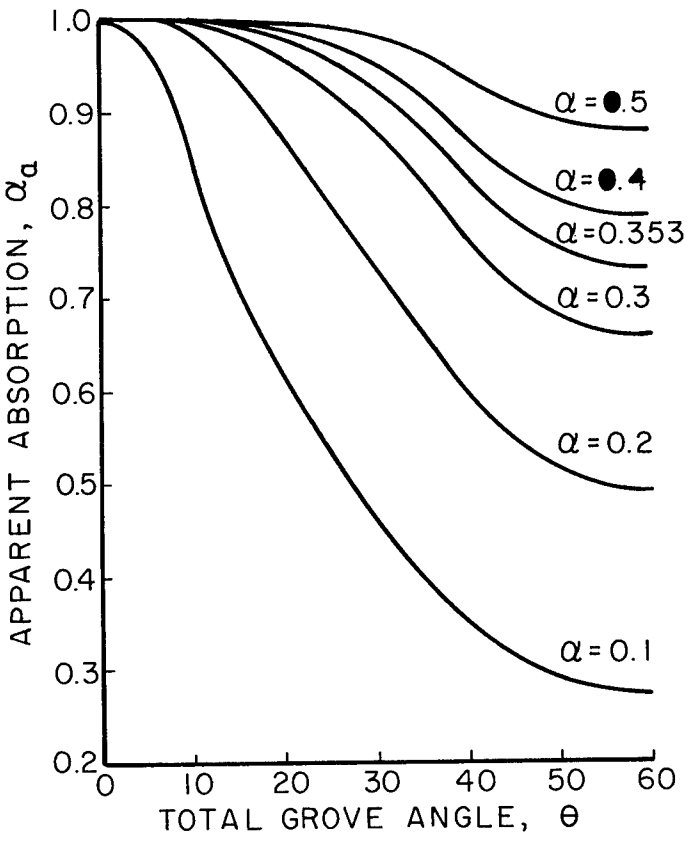

Figure (14) Apparent Absorptance for Normal Incidence for Solar Energy.

model of the experimental finned surface was prepared. The technique described from this point on requires definite dimensions and material properties. In this case the dimension of the fin system was $L_2 = 2$ inches, $L_3 = 2$ inches. The fins were made of thermostatic material supplied by the Metals and Controls Division of Texas Instruments Corporation. This material is completely described in NASA CR-91 (ref. 1). Using the manufacturer's specifications for the material the angle γ or fin movement can be related to the fin temperature T_3. This expression is given in the following equation where T_3 is in °R for fins perpendicular to the spacecraft skin at 610°R (150°F),

$$\gamma = 4.5953 - 0.007535\ T_3 \tag{24}$$

Total configuration factors $F_{ij\ tot}$ as used in equations (16), (17), and (18) depend on the position of the fin given by γ. These values were calculated and from the resulting values a polynomial was used to fit the values. The results of the equation fitting for the script $\mathcal{F}$ values are given in the following equations.

$$\mathcal{F}_{23} = 0.0253 + 0.0732\ \gamma \tag{25}$$

$$\mathcal{F}_{25} = 0.7685 - 0.43076\,\gamma - 1.9805\,\gamma^2 \quad (26)$$

$$\mathcal{F}_{35} = 0.0323 - 0.06168\,\gamma \quad (27)$$

In later work, these expressions have been improved by using a quadratic equation for both $\mathcal{F}_{23}$ and $\mathcal{F}_{25}$.

The actual values of the conductances required for the thermal analysis are nonlinear equations in T_3 and T_2. A typical expression for the conductance is given by equation (28):

$$K_{25\ \text{rad.}} = \mathcal{F}_{25} A_2\, \sigma\, (T_2^2 + T_5^2)(T_2 + T_5)$$

but T_5 is assumed to be $0°R$, e.g.,

$$K_{25\ \text{rad.}} = \mathcal{F}_{25} A_2\, \sigma\, T_2^3$$

or substituting $\mathcal{F}_{25}$ as a function of T_3, using equations (24) and (26),

$$K_{25\ \text{rad.}} = \left[-1.231 \times 10^{-8} + 4.0113 \times 10^{-11}\, T_3 - 3.2086 \times 10^{-14}\, T_3^2\right] T_2^3 \quad (28)$$

In a similar manner $K_{23\ \text{rad.}}$, $K_{35\ \text{rad.}}$, and $K_{34\ \text{rad.}}$ were obtained. In any conductance involved with surface 3 the surface of two fins was considered, i.e., the two fins were lumped as a single node in the model.

A diagramatic representation of the two nodes is shown in Figure 15. Conductances $K_{23\ \text{rad.}}$, $K_{25\ \text{rad.}}$, $K_{35\ \text{rad.}}$, and $K_{34\ \text{rad.}}$ were evaluated as indicated. The two conductances $K_{34\ \text{rad.}}$ and $K_{35\ \text{rad.}}$ can be added into a single conductance since they both connect the same thermal potentials. As explained previously, this was not done in order to make clear the loss of energy from the inner and outer fin surfaces.

The two energy sources $Q_{\text{solar},3}$ and $Q_{\text{solar},2}$ are also functions of the fin temperature T_3. Using equations (21), (22), and (23) with equation (24) the energy sources are evaluated. In this case $Q_{\text{sol.3, inner}}$ and $Q_{\text{sol.3, outer}}$ were added to give $Q_{\text{solar},3}$. The conductance between surfaces 2 and 3 by solid conduction heat transfer was evaluated using the mid-point of the fin as the nodal lump and the entire base area as a nodal lump.

As an example of the results obtained from this thermal model, an analysis was made using a spacecraft skin coating material with terrestial emittance of 0.88 and solar absorptance of 0.248 with the fin inner surface assumed to be vacuum deposited aluminum with constant properties of reflectance and absorptance of 0.93 and 0.07 respectively. The fin outer surface was assumed to have a terrestial emittance of 0.1 and a solar absorptance of 0.353. Solar absorptance was determined from monochromatic reflectance measurements.

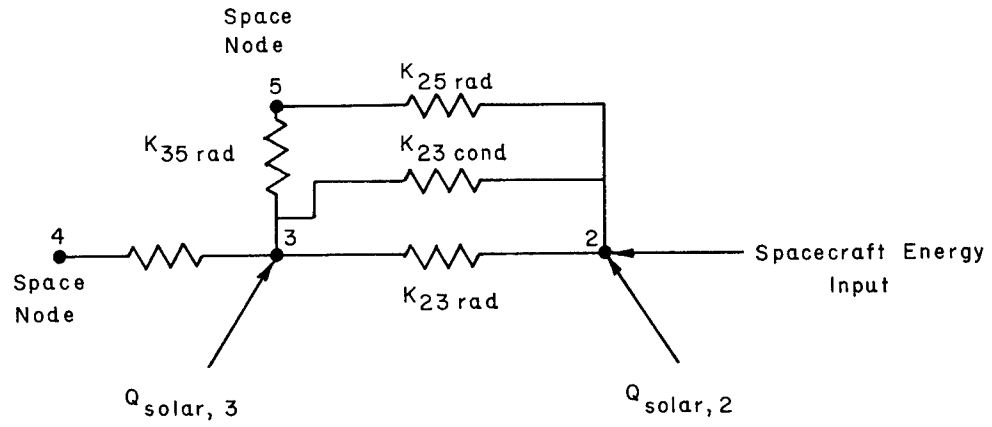

Figure (15) Thermal Model for a Fin System.

With the thermal model as described, the skin temperatures of a fin system oriented such that the solar input was always normal to the surface was calculated. These results for various solar inputs (expressed as sun equivalent) are presented in Figure 16 for two internal heat generation values. In the low power case, 10 Btu/hr-ft^2 or 2.93 watts/ft^2 were assumed to be dissipated and in the high power case 50 Btu/hr-ft^2 or 14.65 watts/ft^2 were used. The base plate temperature for the same power dissipation rates for a white paint surface with $\alpha_s = 0.248$ and $\epsilon_t = 0.88$ are also presented. A comparison of the two curve sets indicate the amount of temperature control possible with the thermal model assumed.

The thermal analysis of the model presented in this discussion indicates that the fins are nearly normal to the surface for all solar inputs other than the low solar inputs. This is reflected in the results for the region from 0.5 sun equivalents to 1.0 sun equivalent. In this region the fin system is entirely passive. At the lower solar inputs the fins begin to move resulting in an active system. This is most strongly indicated by the high power dissipation curve between 0.5 and 1.0 sun equivalents. In the case of the low power dissipation system, the active position of the curve is limited due to the more sudden closing of the fins over the surface, the system again becomes a passive system. This passive system is fairly low, depending on the fin back surface and thermal conductance, emittance surface radiating to space.

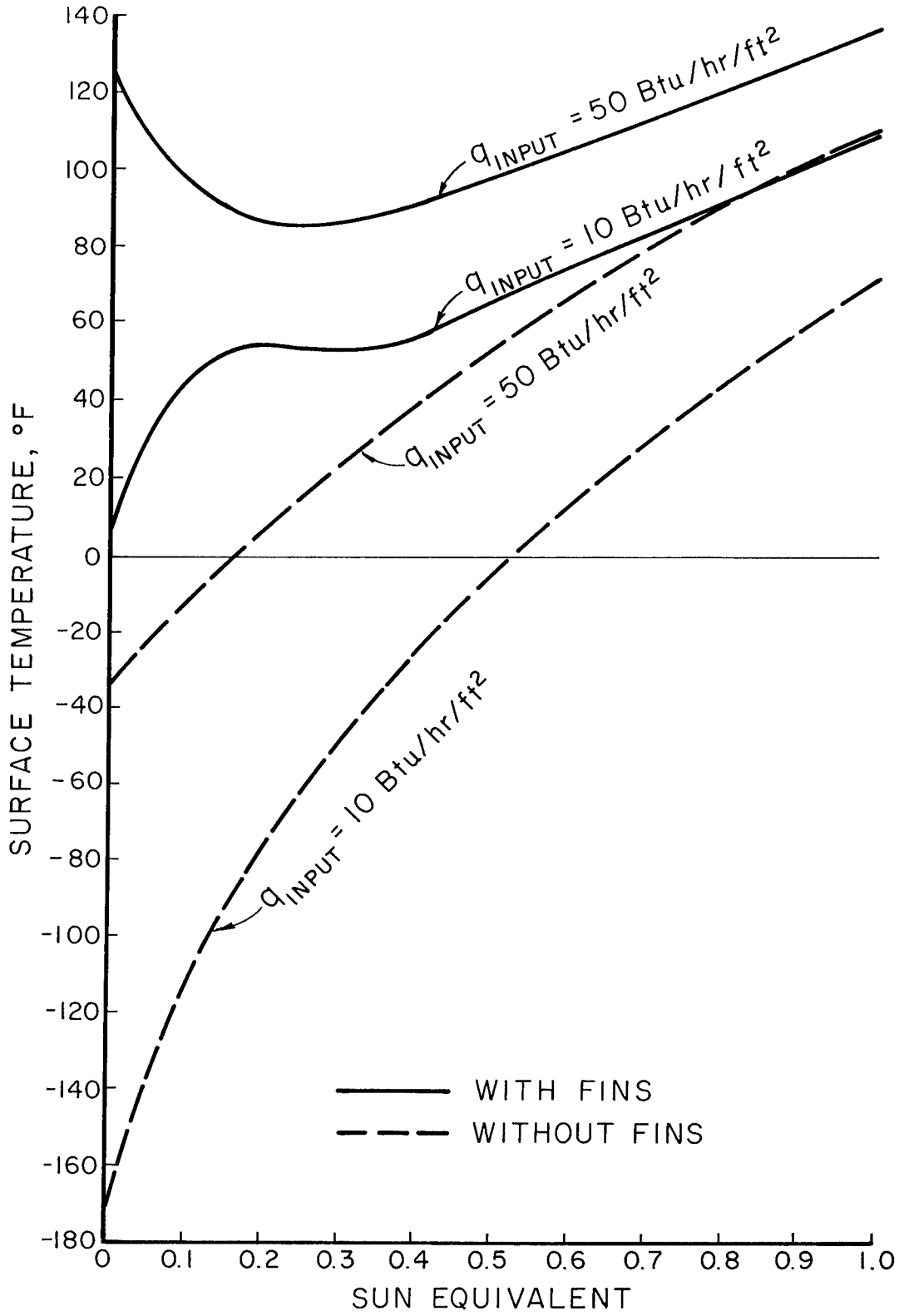

Figure (16) Results of Thermal Analysis.

EXPERIMENTAL SYSTEM

In an attempt to validate the thermal analysis technique, a test model of the finned spacecraft surface was prepared. This test spacecraft surface and the associated test system were described in a previous report to NASA; however, for completeness a portion of the report is repeated herein.

Test Section Construction

In order to prove the analytical results obtained in the previous investigations, a test section was designed for actual testing of the spacecraft system in the simulated outerspace environment. The assumptions on which the previous analysis were based and which had to be met by the model were: (1) the walls must be specularly reflecting walls, (2) the base should be a diffuse white material, and (3) the fins should be straight at about 150°F. From information obtained from the grantor, it was determined that the size of the test system should be approximately 1 square foot. Therefore, a 1 square foot brass plate was chosen as the base upon which to mount the fins. The fins were assumed in the analysis to be constructed of a bimetallic material which consisted of an Invar low-expansion side material and a high-expansion side material which had manganese as the primary alloying ingredient. These fins were assumed to be 0.003 inch thick and for the 1 square foot plate section it was decided the fins should be made 2 inches in length with a spacing of 2 inches between adjacent fin layers. The first problem involved in the construction of the test system was to shape the material in such a way that the fins would be straight or vertical at approximately 150°F. As the material was delivered, it had only a slight longitudinal curvature and a strong crossbow or a curvature in the 2-inch dimension of the material. Initially a rolling device was constructed in the hope that this could be used to shape the fins but rolling did not produce the desired fin shape. Since rolling did not work, a method involving heat treatment was devised and this system was the ultimate system which was used in fin shaping. Basically the heat treatment method consisted of the rigid application of the fin material to a curved mandrel and then heat treating to obtain the proper curvature. Several trials at different temperatures and with different mandrel shapes were made and the final shape was obtained by wrapping the strip tightly around a piece of tube with an outer diameter of about two inches and heating for about two hours at 370°F. This resulted in approximately the correct curvature in the longitudinal direction or the length of the fin material; however, the fin material still had the crossbow in it which had to be removed. After cutting the fins from the long 2-inch wide material, the fins were again wrapped around about a 2-inch diameter mandrel such that the direction of bending was opposite to the direction of the crossflow and they were then heated in this position for an hour at 250°F. These two heat treatments resulted in a fin which had the currect curvature to be used on the test surface. The completed fins were cut into a 2 1/4-inch length and 3/16 of an inch on one end was bent backwards in order to avoid the crossbowing effect which develops as the temperature of the fins increases above the ambient temperature. This is shown in Figure 17 where a typical fin with the upper end bent backward is illustrated. In this case, the connotation of bent backwards means that the fin material was bent in the direction towards the Invar

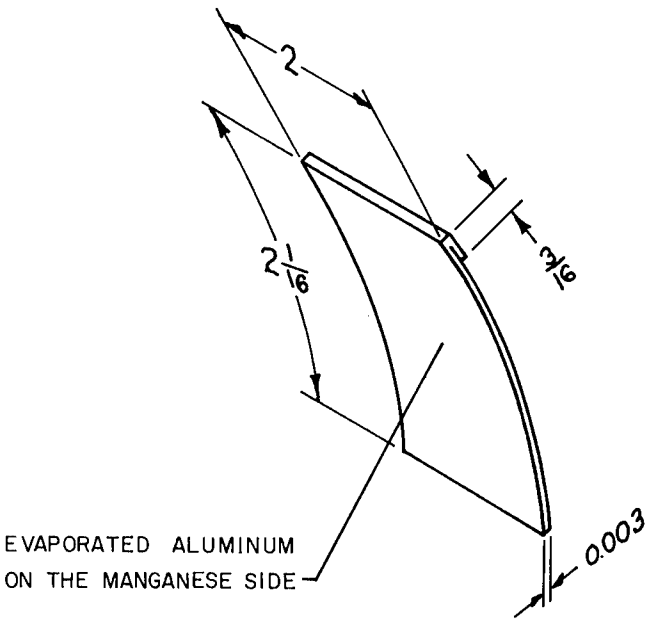

Figure (17) Typical Fin.

side or low-expansion side. The fins as shown in Figure 18 have the bend which they normally would have a room temperature which of course for these fins is a relatively low temperature. After bending the 3/16-inch strip back along the top of the fin, the fin length is 2 1/16 inches of width of which the last 1/16 inch is used for mounting.

Previous investigations reported in the other two progress reports indicated that the reflectance of the high-expansion side was not as high as would be required for the simulation of the analysis; therefore, the high-expansion or manganese side of the fins was vacuum plated with a thin layer of aluminum. This aluminum overcoating was thick enough to be opaque and should result in essentially the reflectance of pure evaporated aluminum on the high-expansion side or the side facing the grooves of the spacecraft system.

The base of the spacecraft surface, a 1 square foot brass plate about 1/8 of an inch thick, was slotted by a milling operation with five slots 2 inches apart approximately 1/16 of an inch deep. Then, two iron-constantan thermocouples were installed by drilling from the back as near to the exposed surface as possible. The back of this plate was coated with a highly absorbing black paint since it would receive energy from the heater plates by radiation. The front side of the plate, the outer or spacecraft surface side, was coated with Cat-a-lac white paint, No. 463-1-500. Characteristics for this exact paint were not available; however, a similar paint from the same manufacturer had been examined experimentally. The characteristics of Cat-a-lac No. 463-1-8 which were used in the analysis are shown in Figure 19. As can be seen from Figure 19, this Cat-a-lac white paint has a relatively low solar absorbtance and a high terrestrial emittance. However, it is not as good as some of the modern white paints now available. In

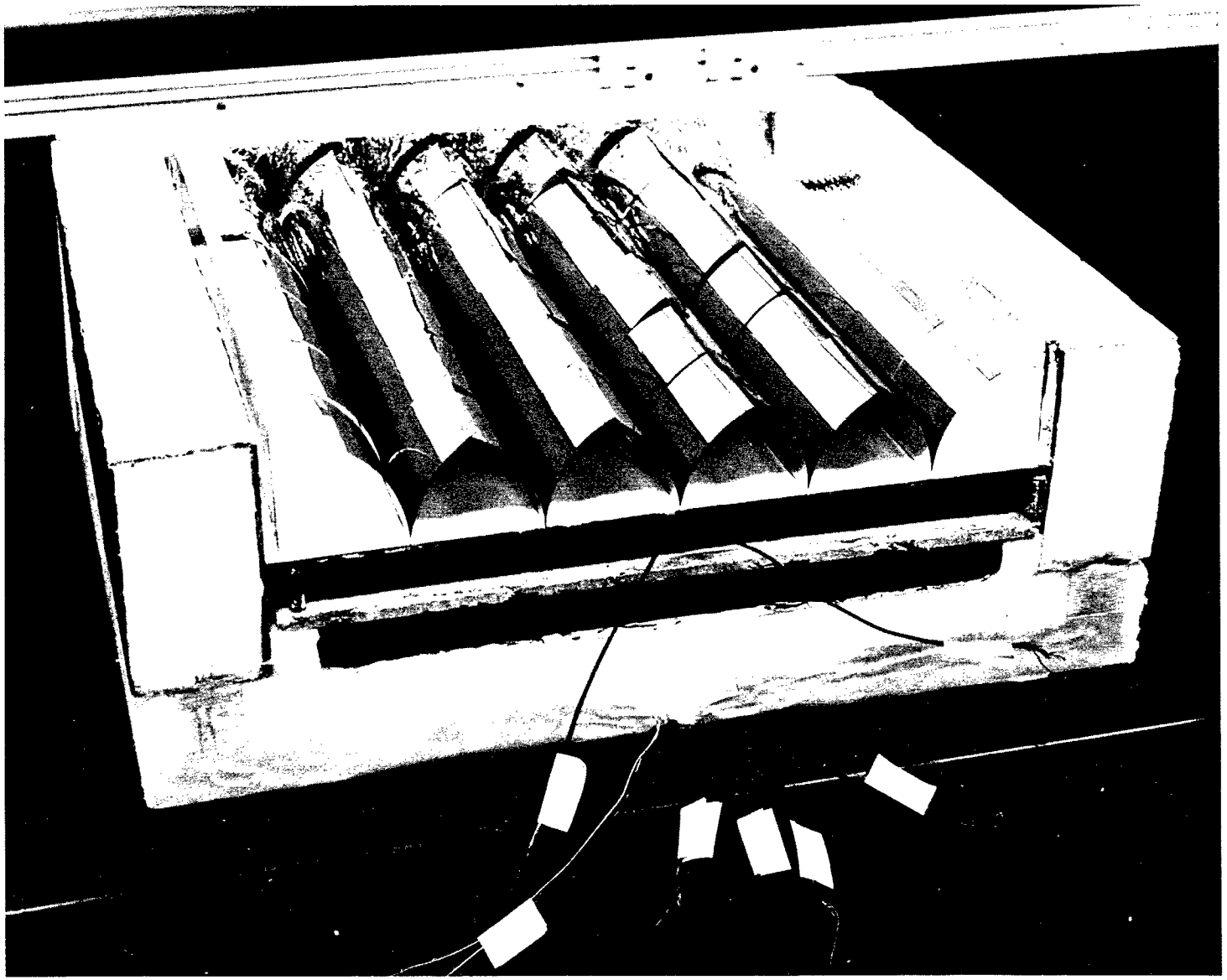

Figure (18) Test System.

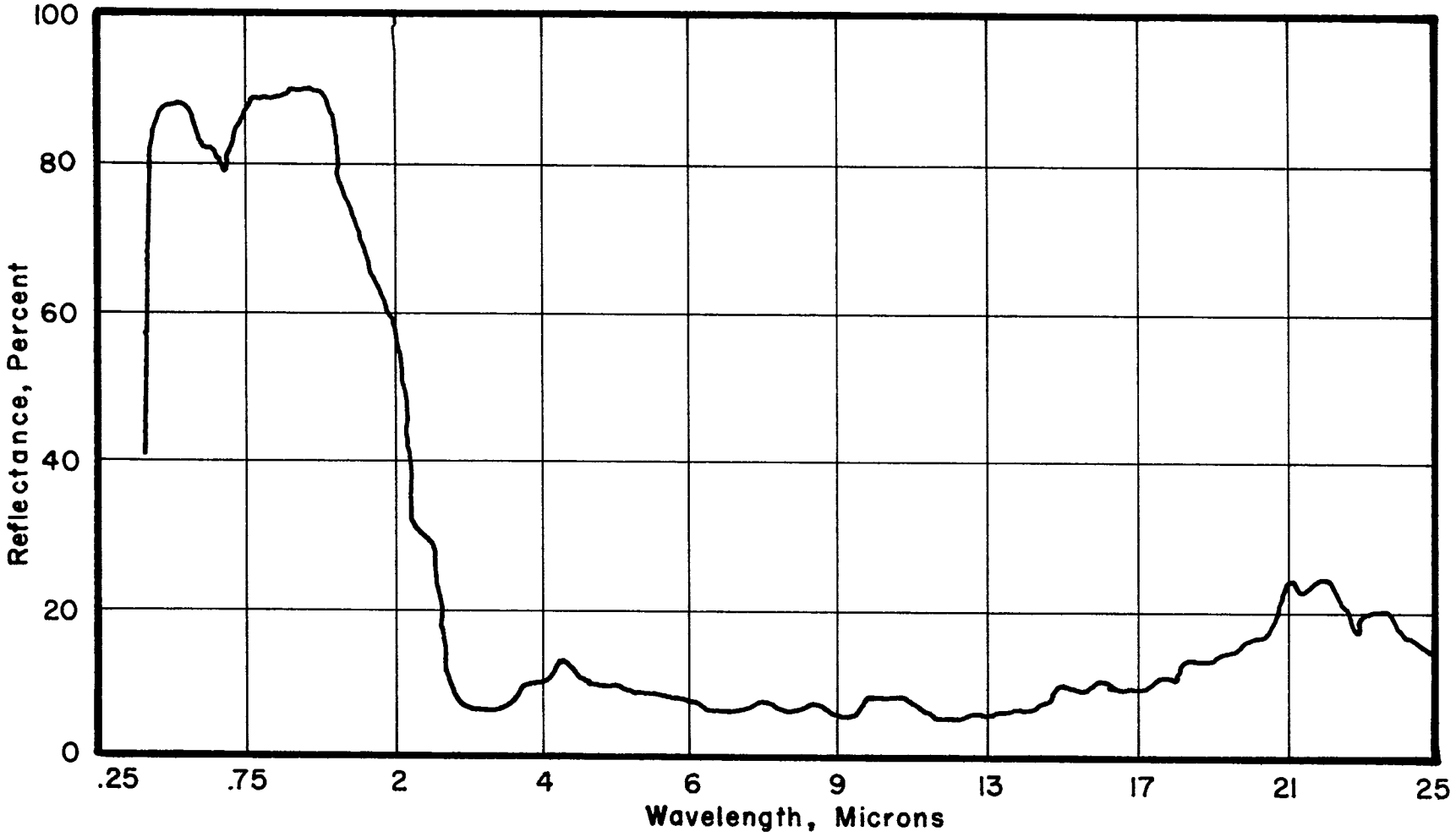

Figure (19) Monochromatic Reflectance of White Epoxy Resin Paint (Cat-a-lac) No. 463-1-8.

the assumptions of the analysis for this system, it was assumed that the white base paint was a diffuse surface; however, the Cat-a-lac white paint gave a slight gloss upon application. Careful sanding was used to remove this gloss, and it is assumed that this does not change the reflectance of the surface. Of course, this is not exactly true; however, the paint was not diffusing enough as applied to approximate the conditions of the analytical work. After the base plate was prepared in this manner, the fins were placed in the slots in the brass plate in their proper positions; and then a small amount of Eastman 910 adhesive was allowed to flow into the space between the fins and the slot edges. This resulted in a strong bond between the fins and the base and is the method suggested for the construction of spacecraft surfaces of this type. A picture of the completed test surface installed in a portion of the required test system is shown in Figure 18. As can be seen, the procedure used in the construction of the test surface resulted in very uniform curvature for the fins and a system which would appear to be very close to the system assumed in the analytical work.

Construction of the Test System

The basic test system is shown in Figure 20. As can be seen from this figure, the test system consists primarily of an insulated box to contain the test surface plus a heat source to simulate the internal heat generation of the spacecraft. Below the heat source a single layer of aluminum foil is used as part of a heat meter to determine the energy transferred from the heater plate through the test system other than through the test surface. The heat source consists of a piece of transite 1/4-inch thick, 1 square foot in size. On the plate is wound the heater element which is made of 30 gage Chromel A heater wire. This resistance wire was chosen such that approximately 40 watts could be dissipated when a potential of 110 volts is applied to the heater windings. The heater windings were placed on the upper face of the transite board and covered with Saureisen electrical cement. In order to control the energy input to the test surface, the heater temperature will be controlled with a proportional controller based on the temperature of the plate. A small bead thermistor temperature sensor was imbedded on the upper side of the plate and covered with Saureisen cement. In order to reduce the amount of energy lost from this plate, the entire lower section of the test system consists of rigid polystyrene blocks covered with aluminum foil. The rigid polystyrene blocks serve both to support the heater assembly and the test surface and to provide insulation between the heated section and the metal wall container for the insulation and test surface. The metal wall container consists of two separate containers with the region between the two containers filled with vermiculite powder. By placing suitable spacers, the inner and outer metal wall containers are thermally insulated away from each other. The outer surface of the metal wall container, that is the outside surface, is covered with aluminum foil cemented on with contact cement on all surfaces except for the surface presumed to be irradiated by the solar simulator. This surface is painted with Cat-a-lac white paint in order to maintain a relatively low temperature in this region.

Directly below the heater plate a single aluminum foil sheet is mounted which serves as a heat meter. This aluminum foil plate actually consists of two sheets of aluminum foil with three thermocouples connected in parallel sandwiched between the two plates, and the two plates are joined by contact cement. This aluminum

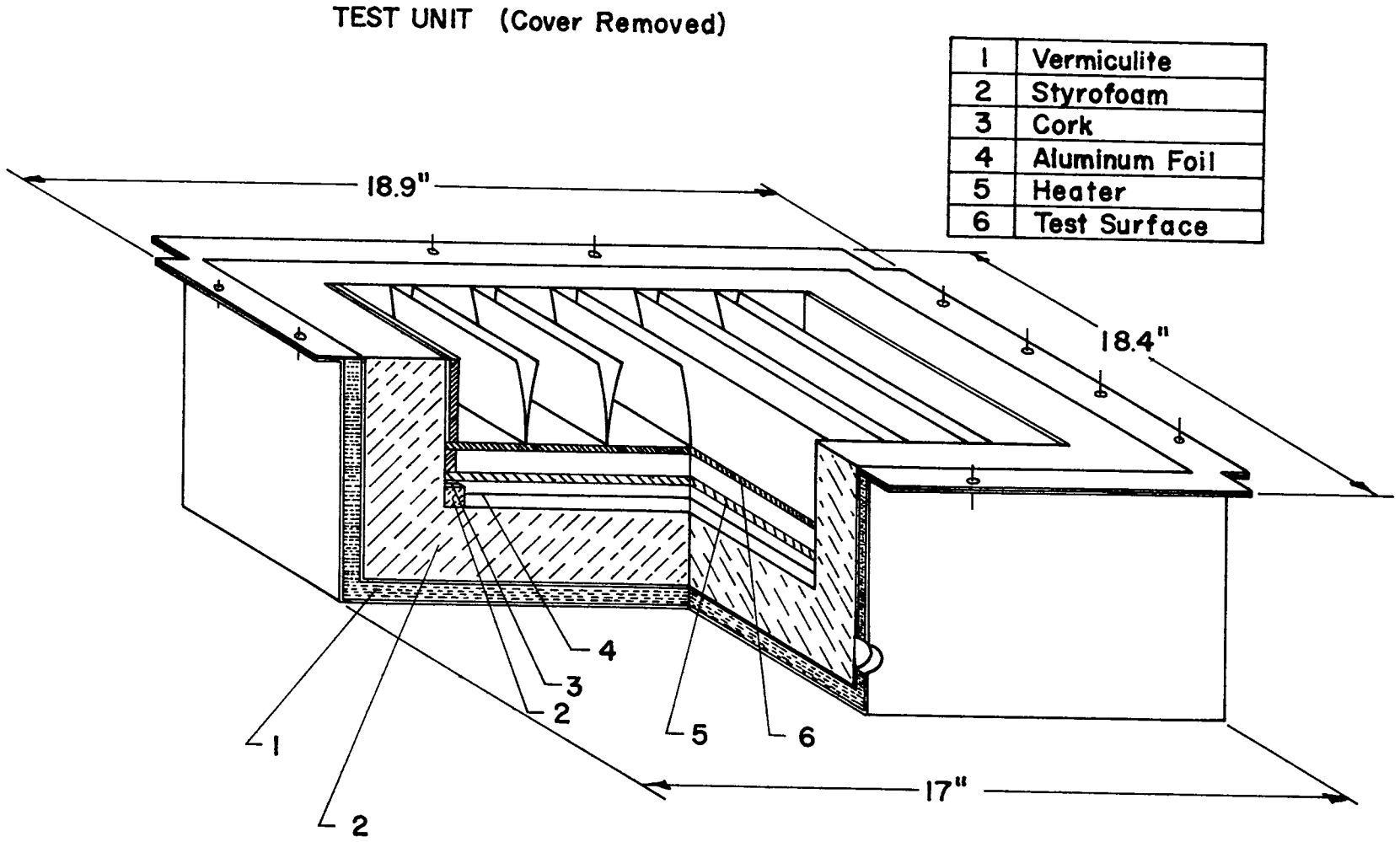
TEST UNIT (Cover Removed)
1 Vermiculite
2 Styrofoam
3 Cork
4 Aluminum Foil
5 Heater
6 Test Surface
18.9"
18.4"
17"
1
2
2
3
4
5
6

Figure (20)

foil radiation shield is directly above a styrofoam insulation block which is also covered with aluminum foil. The outer surface of the styrofoam insulator has installed in it a copper constantan thermocouple such that the temperature of the aluminum foil covering can be determined. In the apparatus built, the spacing between the aluminum foil radiation shield and the aluminum foil on the outer surface of the styrofoam block is approximately 1/2 inch, and these two plates are approximately 1 square foot in size. Two parallel plates with these dimensions very nearly act as two infinite parallel plates. For this reason, the two parallel plates can be used as a heat meter. The basic idea of this heat meter is that the total energy passing in this direction away from the heat plate will be approximately 10 per cent of the total energy generated. Therefore, even through the exact emittance of the two parallel aluminum plates is not known, the estimated value of the emittances will result in energy transfer rates which are perhaps ± 10 per cent of the 10 per cent which goes in this direction. Since about 10 times more energy goes in the direction through the test section, an error of 10 per cent in the evaluation of the energy passing downward from the heater plate will result in about a 1 per cent error in the energy calculated as passing up from the heater plate through the test section. Since the total energy being dissipated by the heater plate is easily measured by electrical methods, the amount of energy passing upward through the test section can be determined with very good accuracy using this system.

As a matter of general interest in evaluating the energy losses from the entire test system, thermocouples are located in numerous positions around the insulating walls.

TEST PROGRAM

The entire test system was installed in a space simulation chamber at Goddard Spaceflight Center under the direction of Mr. Robert Kidwell. This space simulation chamber used a well collimated mercury-zenon solar simulator. In the tests run to date an approximate solar constant of 0.9 and no solar input have been run. It is anticipated that the system will be tested at various power inputs with a variety of solar polar angles in the near future.

All test data to date have been obtained using the temperature controlled heater plate as shown in Figure 20, item 5. This technique was used in an attempt to reduce the thermal lag of individual tests. Since the test section has a relatively small mass, the main thermal lag of the test system is caused by the container and insulation used to direct the energy generated through the test section. By using a controlled heater plate and a radiant heat meter below the plate, an instantaneous power flow through the test section can be determined when the test section has come to equilibrium.

Using this basic technique the following basic test data were obtained:

Table 1

Preliminary Test Data

Test Number	Power Input Watts	Solar Constant Equivalent Suns	Base Plate Temperature, °F
1	11.25	~ 0.90	135
2	19.0	~ 0.90	152
3	26.0	off	99
4	33.0	off	119

Test Number	Nominal Heater Temperature °F	Heat Meter Temperature °F	Opposite Heat Meter Temperature °F
1	155	126	98
2	185	136	92
3	155	85	19
4	185	105	36

From this data is was possible to calculate the various quantities of energy leaving the heater plate in various directions. The initial tests had three main paths for energy flow from the heater plate. These consisted of energy flow by radiant transfer from the heater to the test section, radiant transfer from the heater to the aluminum foil heat meter and conduction transfer from the heater plate through the test section plate out to the surroundings through the transite support pieces. The energy transfer in these three directions for each of the tests were approximated and are listed in Table 2. Since all properties were estimated, these values may be in error by at least ± 25 per cent.

Table 2

Energy Transfer From the Heater

Test Number	Radiant Energy Transfer to the Heat Meter Btu/hr	Radiant Energy Transfer to the Test Section Btu/hr
1	0.89	33.5
2	1.50	56.7
3	1.56	75.9
4	1.80	97.9

Test Number	Conduction Energy Transfer to the Surroundings Btu/hr	Energy Flux Through a Fin System Btu/hr-ft^2
1	4.0	35
2	6.6	59
3	11.2	65
4	13.0	88

The total radiant energy to the test section was dissipated through four 2-inch fin systems which were equivalent to the system described in the Thermal Model section of this report. On each side of the four 2-inch fin systems a 2-inch base plate segment was partially covered by a single fin. When the test section was not irradiated with the solar simulator, these two sections would not be typical fin systems. This is because one side of the 2-inch groove had an active fin wall and the other side was an aluminum foil covered polystyrene insulating block. When the solar simulator was turned on, the fins would assume a near perpendicular wall for the groove, thus the two-edge grooves would be typical systems and can be treated as such. Using these concepts the energy dissipated by the two atypical grooves in the zero solar input runs 3 and 4 were calculated to be 32.8 Btu/hr and 38.9 Btu/hr respectively. With this information, the energy flux through any fin system was calculated for each of the four runs and is given in Table 2.

The calculated values of surface temperature are about 15°F lower than the measured values in tests 1 and 2. This error is believed to be well within experimental errors.

When the solar irradiation was turned off, the values of spacecraft skin temperatures measured for tests 3 and 4 were 99°F and 120°F respectively. In these cases the calculated skin temperatures were very much higher. This error is not within experimental accuracy and is believed to be caused by inability to accurately predict the energy passing through the fin systems. In both of these cases, the experimental test fixture had soaked in the cold environment until the internal temperatures of the insulation were in the range of 50°F to 60°F. These temperatures existed all around the edges of the heater plate. Since these temperatures were not expected, the energy losses were not expected. These losses, although small, become very important in predicting the spacecraft skin temperature with no solar input. When the solar simulator was

operating, the internal temperatures were much higher making these losses much smaller. For this reason, the test results do not agree with the calculated results for the no sun condition.

CONCLUSIONS

As a result of the preliminary tests and calculations it has been concluded that the test apparatus should be changed. This change will be discussed with the NASA representative at Goddard Spaceflight Center before additional tests are run.

It has also been determined that the fins of the system are not thermally coupled to the base plate. This problem will be examined during the next phase of the project. This will be done by considering coatings for the outer surfaces of the fins which will decouple the fins from the solar irradiation and by using shorter fins to improve conduction coupling to the base plate. Several possibilities exist in this system for improvement of the control characteristics. These will be examined both analytically and experimentally in the future.

References

1. Wiebelt, J. A., and J. F. Parmer, "Spacecraft Temperature Control by Thermostatic Fins-Analysis", NASA CR-91, August 1964.

2. Wiebelt, J. A., J. F. Parmer and G. J. Kneissl, "Spacecraft Temperature Control by Thermostatic Fins-Analysis Part II", NASA CR-155, January 1965.

3. Sparrow, E. M. and S. H. Lin, "Absorption of Thermal Radiation in V-Groove Cavities", NASA report on grant NsG-137-61, April 1962.

4. Eckert, E. R. G. and E. M. Sparrow, "Radiative Heat Exchange Between Surfaces with Specular Reflection," Int. J. Heat Mass Transfer, V. 3, pp. 42-54, 1961.

"The aeronautical and space activities of the United States shall be conducted so as to contribute . . . to the expansion of human knowledge of phenomena in the atmosphere and space. The Administration shall provide for the widest practicable and appropriate dissemination of information concerning its activities and the results thereof."

—NATIONAL AERONAUTICS AND SPACE ACT OF 1958

NASA SCIENTIFIC AND TECHNICAL PUBLICATIONS

TECHNICAL REPORTS: Scientific and technical information considered important, complete, and a lasting contribution to existing knowledge.

TECHNICAL NOTES: Information less broad in scope but nevertheless of importance as a contribution to existing knowledge.

TECHNICAL MEMORANDUMS: Information receiving limited distribution because of preliminary data, security classification, or other reasons.

CONTRACTOR REPORTS: Technical information generated in connection with a NASA contract or grant and released under NASA auspices.

TECHNICAL TRANSLATIONS: Information published in a foreign language considered to merit NASA distribution in English.

TECHNICAL REPRINTS: Information derived from NASA activities and initially published in the form of journal articles.

SPECIAL PUBLICATIONS: Information derived from or of value to NASA activities but not necessarily reporting the results of individual NASA-programmed scientific efforts. Publications include conference proceedings, monographs, data compilations, handbooks, sourcebooks, and special bibliographies.

Details on the availability of these publications may be obtained from:

SCIENTIFIC AND TECHNICAL INFORMATION DIVISION

NATIONAL AERONAUTICS AND SPACE ADMINISTRATION

Washington, D.C. 20546